THE JOURNAL OF BIOLOGICAL CHEMISTRY
Vol. 280, No. 5, Issue of February 4, pp. 3159–3165, 2005

Printed in U.S.A.

Aluminum Triggers Decreased Aconitase Activity via Fe-S Cluster Disruption and the Overexpression of Isocitrate Dehydrogenase and Isocitrate Lyase

A METABOLIC NETWORK MEDIATING CELLULAR SURVIVAL*

Received for publication, October 22, 2004, and in revised form, November 10, 2004
Published, JBC Papers in Press, November 17, 2004, DOI 10.1074/jbc.M411979200

Jeffrey Middaugh‡, Robert Hamel§, Gael Jean-Baptiste‡, Robin Beriault‡, Daniel Chenier‡, and Vasu D. Appanna‡¶

From the ‡Department of Chemistry and Biochemistry, Laurentian University, Sudbury, Ontario P3E 2C6, Canada and §Northern Centre for Biotechnology and Clinical Research, Sudbury, Ontario P3E 6B4, Canada

Although aluminum is known to be toxic to most organisms, its precise biochemical interactions are not fully understood. In the present study, we demonstrate that aluminum promotes the inhibition of aconitase (Acn) activity via the perturbation of the Fe-S cluster in *Pseudomonas fluorescens*. Despite the significant decrease in citrate isomerization activity, cellular survival is assured by the overexpression of isocitrate lyase and isocitrate dehydrogenase (IDH)-$NADP^+$. ^{13}C NMR spectroscopic studies, Blue Native PAGE, and Western blot analyses indicated that although the decrease in Acn activity is concomitant with the increase of aluminum in the culture, the amount of Acn expressed is not sensitive to the concentration of the trivalent metal. A 6-fold decrease in Acn activity and no discernable change in protein content in aluminum-stressed cultures were observed. The addition of $Fe(NH_4)_2(SO_4)_2$ in a reducing environment led to a significant recovery in Acn activity. This enzymatic activity reverted to normal levels when aluminum-stressed cells were transferred to either a control or an iron-supplemented medium. The overexpression of the two isocitrate-metabolizing enzymes isocitrate lyase and IDH-$NADP^+$ appears to mitigate the deficit in Acn activity. The levels of these enzymes are dependent on the aluminum content of the culture and appear to be under transcriptional control. Hence, the regulation of the enzymes involved in the homeostasis of isocitrate constitutes a pivotal component of the global metabolic strategy that ensures the survival of this organism in an aluminum citrate environment.

Metabolism is the foundation of all living organisms, and any biological function is the manifestation of the global cellular metabolism. Hence, any cellular behavior is a direct or indirect product of its metabolism. The enzymes/metabolites participating in metabolism provide a precise snapshot of a cellular phenotype (1, 2). As part of our study on molecular adaptation, we have uncovered an interesting model system that allows deciphering the metabolic reconfiguration evoked by metal stress. The metal toxicant was supplied to the microbe *Pseudomonas fluorescens*, complexed to citrate, the only carbon source. The role of oxalate and phosphatidylethanolamine in the immobilization of aluminum has been demonstrated recently (3, 4). It appears that the cellular metabolism is reconfigured with the aim of providing the metabolic precursors that allow for the survival of the organism in an aluminum environment. Hence, an aluminum-adapted phenotype with an entirely different set of metabolic pathways than in the wild type is promoted.

Citrate, the sole carbon source utilized in this system, is known to be cleaved in various organisms, primarily by the enzymes citrate-lyase (CL),[1] ATP-citrate-lyase (ATP-CL), and Acn. Whereas CL mediates the cleavage of citrate to acetate and oxaloacetate, ATP-CL catalyzes the degradation of tricarboxylic acid into acetyl-CoA and oxaloacetate (5, 6). The latter is also referred to as a lipogenic enzyme, because it participates in the generation of acetyl-CoA, a key precursor in the biosynthesis of fatty acid, and is regulated via the phosphorylation/dephosphorylation of its histidine residues (7, 8). CL, on the other hand, is usually invoked by microorganisms utilizing citrate in anoxic environments (9). Aconitases, the other group of enzymes that are involved in the metabolism of citrate, are Fe-S proteins having a predominantly [4Fe-4S] cluster in the enzymatically active form. They catalyze the reversible isomerization of citrate to isocitrate, a key step in the tricarboxylic acid cycle. The isocitrate is metabolized subsequently by IDH-NAD^+ to give α-ketoglutarate and NADH. Acn is sensitive to the oxygen gradient and the cellular iron status (10). These two factors play an important role in the reactivity of Acn. In mammalian systems, Acn with a [3Fe-4S] cluster serves as a regulatory protein that controls the stability and translation of mRNAs encoding proteins involved in iron and energy homeostasis (11, 12). The regulatory Acn, referred to as iron-responsive proteins, binds to the iron-responsive elements localized in the RNA-stem-loop.

Aluminum is the most abundant metal in the environment and is known to be toxic to all organisms. It may substitute for such metals as iron and calcium and consequently help destabilize biological activity. There are accumulating reports (13) that suggest that aluminum interferes with iron homeostasis

* This work was supported by funding from Industry Canada and Human Resources Development Canada. The costs of publication of this article were defrayed in part by the payment of page charges. This article must therefore be hereby marked "*advertisement*" in accordance with 18 U.S.C. Section 1734 solely to indicate this fact.

¶ To whom correspondence should be addressed: Dept. of Chemistry and Biochemistry, Laurentian University, 935 Ramsey Lake Rd., Sudbury, Ontario P3C 2C6, Canada. Tel.: 705-675-1151 (ext. 2112); Fax: 705-675-4844; E-mail: vappanna@laurentian.ca.

[1] The abbreviations used are: CL, citrate-lyase; Acn, aconitase; IDH, isocitrate dehydrogenase; ICL, isocytrate lyase; DTT, dithiothreitol; CFE, cell-free extract; BN, Blue Native; BisTris, 2-[bis(2-hydroxyethyl)-amino]-2-(hydroxymethyl)propane-1,3-diol; Tricine, *N*-[2-hydroxy-1,-1-bis(hydroxymethyl)ethyl]glycine.

and severely impedes cellular metabolism. Aluminum also is known to favor the generation of an oxidative environment because of its ability to create a labile iron pool and to interact with membrane lipids (14). Although most organisms succumb to the toxic influence of aluminum, some living systems are known to elaborate intricate strategies to fend off the dangers associated with an aluminum-rich environment (15, 16). We have shown the ability of *P. fluorescens* to tolerate millimolar amounts of aluminum complexed to citrate, the only carbon source (17). The present study was aimed at elucidating the enzymes involved in the metabolism of citrate in the presence of aluminum. Here we have shown that aluminum severely inhibits Acn activity by perturbing the Fe-S cluster and that the degradation of citrate is aided by two downstream enzymes, ICL and IDH-$NADP^+$. The overexpression of ICL and IDH contributed effectively in the metabolism of the tricarboxylic acid even under markedly diminished Acn activity. It appears that the rapid cleavage of isocitrate, the product generated by Acn, via ICL and IDH provided an efficient route for the survival of this organism in an aluminum citrate environment. The significance of this aluminum-evoked metabolic shift is discussed, and the pivotal role of a metabolic circuit operative in this organism is explained.

EXPERIMENTAL PROCEDURES

Bacterial Culture and Cell-free Extracts—P. fluorescens, ATCC 13525, was maintained (on 2% agar) and grown in a mineral medium consisting of Na_2HPO_4 (6.0 g), KH_2PO_4 (3.0 g), NH_4Cl (0.8 g), $MgSO_4$ (0.2 g), and citric acid (4.0 g/liter deionized distilled water). Trace elements ($FeCl_3 \cdot 6H_2O$ (2 μM), $MgCl_2 \cdot 4H_2O$ (1 μM), $Zn(NO_3)_2 \cdot 6H_2O$ (0.05 μM), $CaCl_2$ (1 μM), $CoSO_4 \cdot 7H_2O$ (0.25 μM), $CuCl_2 \cdot 2H_2O$ (0.1 μM), and $NaMoO_4 \cdot 2H_2O$ (0.1 μM)) were also added. In the aluminum-stressed medium, citric acid was complexed with $AlCl_3$ in a ratio of 19 mM citrate to 15 mM $AlCl_3$. The pH was adjusted to 6.8 with dilute NaOH and 200-ml amounts of media were dispensed in 500-ml Erlenmeyer flasks. Inoculations were made with 1 ml of stationary phase cells grown in a medium unamended with the test metal and aerated on a gyratory water bath shaker, model 76 (New Brunswick Scientific) at 26 °C. When other test metals were utilized, the citrate concentration was also 19 mM, and gallium, calcium, and iron were present at 1, 5, and 5 mM concentrations, respectively. In the glucose cultures, 19 mM hexose was utilized. Cells were collected by centrifugation (10,000 × *g* for 10 min at 4 °C) and washed twice with 0.85% NaCl and once with cell storage buffer (100 mM Tris-HCl (pH 7.3), 1 mM DTT, and 1 mM phenylmethylsulfonyl fluoride). Cells were disrupted ultrasonically in the cell storage buffer containing 10 mM tricarballylic acid, using a New Brunswick Scientific sonicator at power level 4 for 15 s at four intervals. The unbroken cells were separated from the cell-free extract (CFE) by centrifugation at 3000 × *g* for 5 min at 4 °C. The supernatant fraction of the CFE was collected and centrifuged at 180,000 × *g* for 60 min at 4 °C to yield membrane and soluble components. The soluble fraction was further centrifuged at 180,000 × *g* for 2 h to afford a membrane-free system. Fractions were kept on ice in the refrigerator or frozen at −20 °C for storage up to a maximum of 4 weeks. Protein concentrations were measured by the Bradford method, using bovine serum albumin as a standard (18).

Enzyme Assays—The soluble fractions (400 μg of protein equivalent) were incubated at room temperature in a 2-ml reaction containing 100 mM Tris-HCl (pH 7.3), 1 mM DTT, 1 mM phenylmethylsulfonyl fluoride, 10 mM citrate or metal citrate complexes, and 20 mM malonate. Acn activity was monitored by following the formation of *cis*-aconitate at 240 nm (ϵ = 3600 M^{-1} $liter^{-1}$) (19). ICL activity was monitored by measuring glyoxylate formation with the aid of 2,4-dinitrophenylhydrazine (20). 400 μg of protein equivalent and 2 mM isocitrate were used in the same buffer system. Glyoxylate was utilized as the standard. IDH-$NADP^+$ was analyzed in a 1-ml reaction mixture containing 25 mM Tris-HCl (pH 7.3), 5 mM $MgCl_2$, 2 mM isocitrate, 4 mM malonate, and 0.2 mM $NADP^+$. Enzyme activity was monitored by following the formation of NADPH at 340 nm (ϵ = 6400 M^{-1} $liter^{-1}$) for 60 s and by quantitating the α-ketoglutarate formation colorimetrically with 2,4-dinitrophenylhydrazine. α-Ketoglutarate was used as the standard. To monitor the combined activities of Acn and ICL, the soluble fractions were incubated with citrate, and the production of glyoxylate was quantitated. Similarly, to monitor the combined activities of Acn, ICL, and IDH-$NADP^+$ the production of total keto acids (glyoxylate and α-ketoglutarate) was quantitated.

^{13}C NMR Spectroscopy—^{13}C NMR analyses were performed using the Varian Gemini 2000 spectrometer operating at 50.31 MHz for ^{13}C. Reactions were assayed in phosphate buffer (10 mM phosphate, 5 mM $MgCl_2$ (pH 7.3)) with soluble fraction (3 mg of protein equivalent), 5 mM $^{13}C_{2,4}$-labeled citric-2,4-$^{13}C_2$ acid or Al-citric-2,4-$^{13}C_2$ acid. The reactions were performed in 1.5-ml microcentrifuge tubes for 1 h and were stopped by placing the tubes in a boiling water bath for 3 min. Precipitates (if formed) were removed by centrifugation at 20,000 × *g* for 20 min. 600-μl aliquots of the supernatants were mixed with 100 μl of D_2O (99% deuterium). Mixtures were scanned for 20,000 transients, and resulting signals were referenced to standard metabolite spectra.

Blue Native PAGE, SDS-PAGE, Western Blot Analyses, and Activity Stains—Blue Native (BN) PAGE was performed according to the method of Schagger (21). The Bio-Rad MiniProtean™ 2 system was utilized, and gels with a linear gradient (10–16%) were selected to separate the proteins. Soluble protein samples were prepared in BN buffer (50 mM BisTris, 500 mM ϵ-aminocaproic acid (pH 7.0)), and 80 μg of protein/lane was loaded into each well. Gels were electrophoresed under BN conditions. 80 V was used for the stacking gel and was increased to 200 V when the proteins reached the separating gel. The blue cathode buffer (50 mM Tricine, 15 mM BisTris, 0.02% Coomassie Blue G-250 (pH 7.0) at 4 °C) was changed to the colorless cathode buffer (50 mM Tricine, 15 mM BisTris (pH 7.0) at 4 °C) once the running front reached halfway through the separating gel. Electrophoresis was stopped before the running front was out of the gel. The gels were placed subsequently in an equilibration buffer (25 mM Tris-HCl (pH 7.6), 5 mM $MgCl_2$) for 15 min. Acn activity was visualized by the formation of formazan via phenazine methosulfate and NADPH, using an enzyme-coupled assay consisting of equilibration buffer, 5 mM citrate, 0.5 mM $NADP^+$, 5 units/ml IDH (Sigma), 0.4 mg/ml iodonitrotetrazolium, and 0.2 mg/ml phenazine methosulfate. ICL was detected with the same technique except glyoxylate (5 mM) and succinate (5 mM) were the substrates. This enzyme was also detected by staining for glyoxylate generated after the cleavage of isocitrate. Lactate dehydrogenase was utilized as the coupling enzyme (22). IDH activity was visualized with isocitrate (5 mM), $NADP^+$ (0.5 mM), phenazine methosulfate, and iodonitrotetrazolium. Two- and three-dimensional PAGE was performed under the same conditions as described above.

Protein content was analyzed by Coomassie Blue stain and Western blotting techniques. SDS-PAGE using a discontinuous buffer system was performed according to the method of Laemmli (23). A 10% gel and 0.1% SDS were used. Samples were solubilized in 62.5 mM Tris-HCl (pH 6.8), 2% SDS, 10% glycerol, and 2% β-mercaptoethanol at 100 °C for 5 min. Electrophoresis was carried out at a constant 200 V, and slab gels were fixed, stained, and destained according to standard procedures. Immunoblots were performed on single and multidimensional BN gels as well as SDS gels. Briefly, following the completion of one-dimensional BN-PAGE/two-dimensional BN-PAGE or one-dimensional BN-PAGE/two-dimensional SDS-PAGE, the gel was equilibrated in protein transfer buffer (25 mM Tris, 200 mM glycine, 20% methanol) for 10 min. Hybond™-P polyvinylidene difluoride membrane was utilized for electroblotting. The nonspecific binding sites were blocked by incubating the membranes with 5% nonfat skim milk in TTBS (20 mM Tris HCl, 0.8% NaCl, 1% Tween 20 (pH 7.6)) for 1 h. The membranes were then probed with the primary polyclonal antibody specific for native or denatured aconitase (kindly provided by Dr. R. Eisenstein, University of Wisconsin, Madison, WI) and denatured ICL (obtained from Dr. K. Honer Zu Bentrup, Cornell University, Ithaca, NY). The secondary antibody consisted of horseradish peroxidase-conjugated mouse anti-rabbit. The detection of the desired proteins was achieved with the ECL Plus system (Amersham Biosciences). Following a 5-min incubation at room temperature, the blots were visualized with autoradiography film, Hyperfilm™ ECL (Amersham Biosciences). Band intensity was quantified using SCION software (SCION Corporation, Frederick, MD).

Time Profile, Aluminum Dependence, and Expression of Acn, IDH, and ICL—Cells were grown and obtained as described previously. Cells were harvested at various time intervals, and the soluble fractions were isolated. The activities and the protein content of Acn, ICL, and IDH were analyzed by BN-PAGE, SDS-PAGE, and Western blotting. To evaluate the influence of aluminum on these enzymes, cells were cultured in media supplemented with varying concentrations (0, 1.0, 5.0, 10.0, and 15.0 mM) of aluminum. The activities and concentrations of the enzymes were monitored subsequently.

Regulation of Enzymatic Activities and Expression—10 mg of protein equivalent of aluminum-stressed cells were transferred to various citrate media supplemented with 25 μM Fe, 15 mM H_2O_2, rifampicin, and

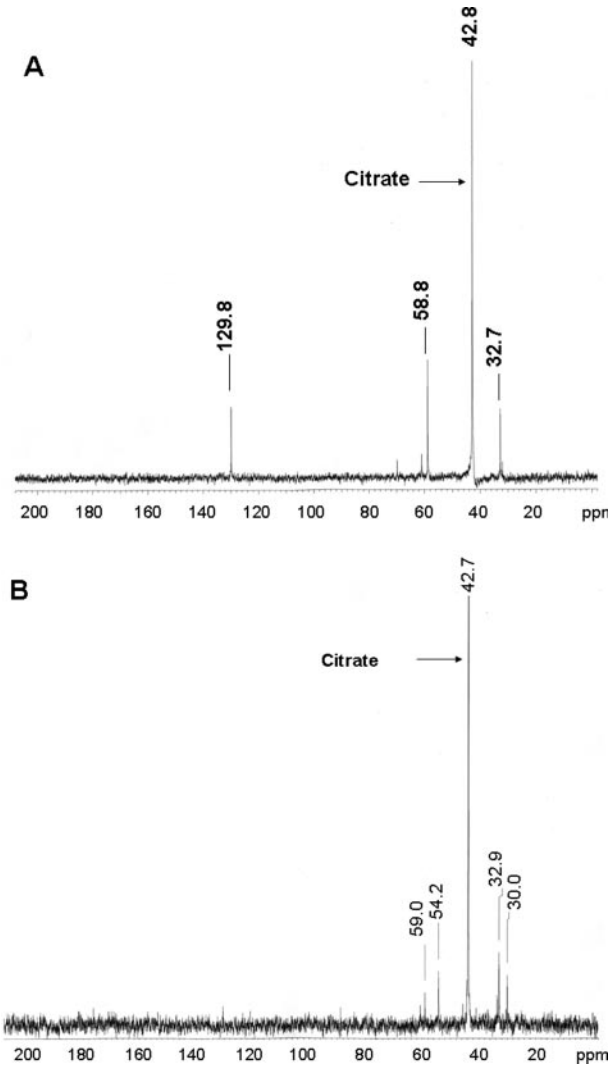

FIG. 1. **Proton-decoupled ^{13}C NMR spectra of soluble fraction of CFE (2 mg of protein) incubated with citric-2,4-$^{13}C_2$ acid (5 mM) for 1 h.** *A*, soluble CFE is shown from cells unamended with aluminum. *B*, soluble CFE is shown from aluminum-stressed cells in the presence of $NADP^+$.

chloramphenicol, respectively. Similar experiments were performed with control cells transferred to aluminum medium. Following an incubation of 6–8 h, cells were harvested, and the soluble cellular extracts were assayed for enzymatic activities and protein concentrations.

In Vitro Reactivation of Acn and Identification of Fe-S Cluster—The reactivation of Acn was performed with 1 mg of protein equivalent of soluble CFE in the presence of 10 mM DTT and 0.5 mM $Fe(NH_4)_2(SO_4)_2$ in the cell storage buffer. The reaction mixture was incubated for 5 min, and Acn activity was monitored. The nature of the Fe-S cluster was studied by scanning 5 mg/ml protein equivalent of soluble CFE obtained from cultures with varying concentrations of aluminum with an Ultraspec 3000 spectrophotometer. In addition, soluble CFE isolated from aluminum cultures transferred to the control medium was also examined. The Fe-S cluster band at 395–420 nm was analyzed (24, 25).

RESULTS

Effect of Aluminum on Acn Activity and Expression—We demonstrate that in the presence of aluminum the ability of Acn to metabolize citrate to isocitrate was hindered. Fig. 1*A* shows that when soluble CFE from cells grown in media unamended with the test metal was incubated with citric-2,4-$^{13}C_2$ acid for 1 h, Acn was able to convert citrate to *cis*-aconitate. This was indicated by the presence of the olefinic C_2 present in *cis*-aconitate showing a distinct signal at 129 ppm (26). However, when soluble CFE from cells grown in the presence of aluminum was used, the signal at 129 ppm was absent, demonstrating that the presence of aluminum in the culture had a negative effect on Acn activity (data not shown). However, if the same reaction was left longer or in the presence of $NADP^+$, the tricarboxylic acid was further metabolized (Fig. 1*B*). Activity staining of Acn on one- and two-dimensional BN-PAGE was used to confirm this apparent decrease in Acn activity. The lack or slight production of formazan in the lane containing soluble CFE from aluminum-stressed cells indicated that this enzyme was severely impeded in these cultures (Fig. 2). To determine whether the lack of Acn activity found in the aluminum-stressed cells was caused by a down-regulation of protein synthesis, Western blot analyses were performed using both one- and two-dimensional BN-PAGE. The protein levels of Acn were

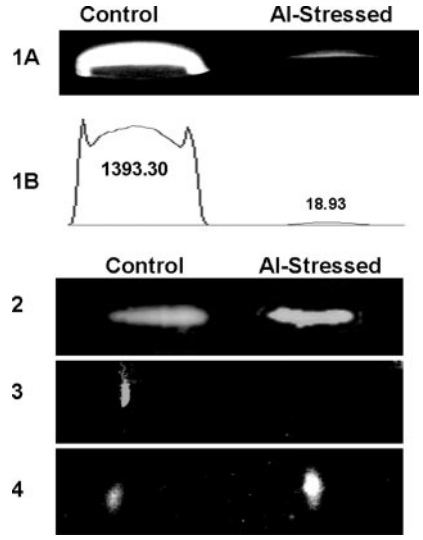

FIG. 2. **Effect of aluminum on activity and expression of Acn.** Activity stains and immunoblots of Acn on one- and two-dimensional BN-PAGE are shown. *Panel 1A*, one-dimensional activity stain; *panel 1B*, band intensity quantification of *1A* using SCION image software; *panel 2*, one-dimensional immunoblot; *panel 3*, two-dimensional activity stain; *panel 4*, two-dimensional immunoblot.

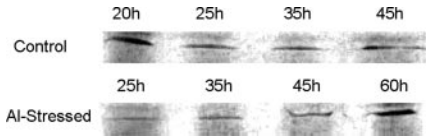

FIG. 3. **Acn activity at different growth intervals.** Activity staining of soluble CFE for Acn on BN-PAGE is shown. Note that the time intervals correspond to similar growth phases.

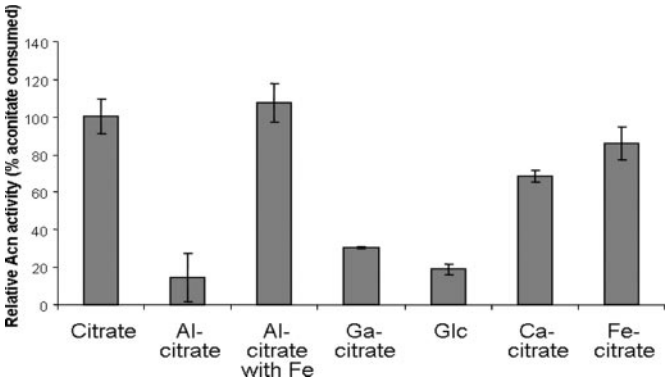

FIG. 4. **Acn activity in cells obtained in various growth media.** Soluble extracts from cells grown in various carbon sources were monitored for Acn activity. Values are mean ± S.D., $n = 3–6$. 100% = 0.124 $\mu mol \cdot min^{-1} \cdot mg\ prot^{-1}$.

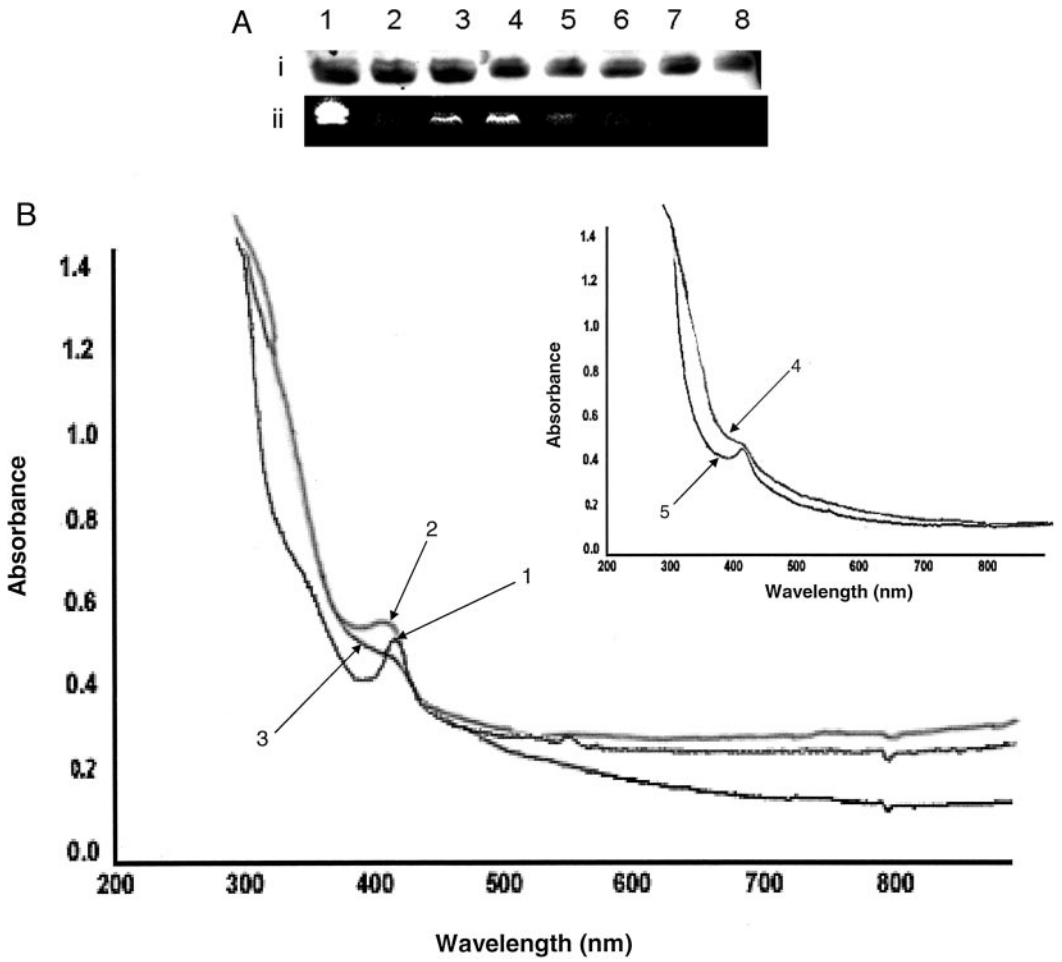

FIG. 5. **Influence of iron and oxidative stress on Acn activity and the Fe-S cluster integrity.** *A*, immunoblot for Acn (*i*) and activity staining of soluble CFE for Acn on BN-PAGE (*ii*) are shown. *Lanes 1*, control; *2*, aluminum-stressed; *3*, cells from aluminum-stressed media transferred to control media; *4*, cells from aluminum-stressed media transferred to control media with 25 μM Fe; *5*, cells from control media transferred to aluminum-stressed media; *6*, cells from control media transferred to media with 15 mM H_2O_2; *7*, cells from control media transferred to aluminum-stressed media containing rifampicin; *8*, cells from control media transferred to aluminum-stressed media containing chloramphenicol. *B*, UV-visible wave scans of soluble CFE are shown. *Traces 1*, CFE from control cultures; *2*, CFE from 5 mM aluminum-stressed cultures; *3*, CFE from 15 mM aluminum-stressed cultures. Note that the markedly diminished band at 395–420 nm is indicative of Fe-S cluster perturbation in aluminum-stressed CFE (24, 25). *Inset*, CFE from 15 mM aluminum-stressed cultures (*trace 4*); CFE from cells grown in 15 mM aluminum media transferred to control media for 8 h (*trace 5*).

observed to be similar if not slightly higher in aluminum-stressed cells, thus, indicating that the change in activity was not because of disparate protein expression (Fig. 2).

Acn Activity in Control and Aluminum-stressed P. fluorescens, Influence of Time of Incubation and Aluminum Concentration—Acn activity was monitored at different time intervals by activity staining on BN-PAGE (Fig. 3). No significant change in Acn activity was evident after 20 h of growth in cells cultured in control medium. The aluminum-stressed cells showed a decrease in Acn activity up to 45 h. However, after 45 h of incubation (the growth phase coincides with the immobilization of aluminum as a phosphatidylethanolamine- and oxalic acid-containing residue (3)), a marked increase in Acn activity was observed. The maximal deficiency in Acn activity was observed in cells subjected to 10–15 mM Al. Cells grown with 0.1–1 mM Al showed no obvious decrease in Acn activity. At a concentration of 5 mM Al there was a noticeable change in Acn activity. However, the presence of iron appeared to have a beneficial effect on this enzyme. These observations were further confirmed by monitoring the formation of aconitate at 240 nm (data not shown).

Acn in Media with Different Metals and Substrates—To determine whether the dramatic decrease in Acn activity was specific to the toxic influence of aluminum, the cells were grown in various media containing different metals complexed to citrate and glucose as the sole carbon source, respectively. As shown by NMR and activity staining, Acn activity in aluminum-stressed cells was reduced drastically. Spectrophotometric analysis pointed to a 6-fold decrease of Acn activity in the aluminum-stressed cells (Fig. 4). Likewise, when Ga^{3+}, another known pro-oxidant metal, was complexed to citrate, a 3-fold decrease in Acn activity was observed. However, when Fe^{3+} complexed to citrate was the substrate, there was no significant perturbation in Acn activity. In fact, Fe^{3+} (1 mM) did reverse the negative trend observed under aluminum-stress. When redox-inactive Ca^{2+} was the test metal, only a slight diminution in Acn activity was evident. Interestingly, when glucose was utilized as the source of carbon, a dramatic 5-fold decrease in Acn activity was observed compared with the control citrate medium.

Regulation of Enzymatic Activity and Protein Expression—To further evaluate the notion that aluminum was the effector resulting in a decrease in Acn activity, cells were subjected to aluminum and then transferred to various citrate media containing aluminum, H_2O_2, iron, chloramphenicol, and rifampicin, respectively (Fig. 5*A*). The cells were subsequently incubated for 8 h. The aluminum-stressed cells experienced an obvious increase in Acn activity in the cultures containing

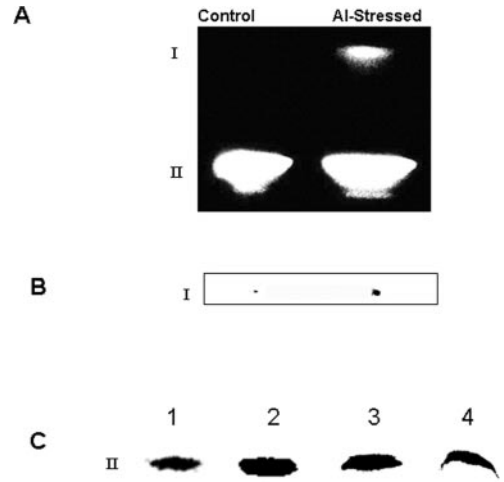

FIG. 6. **Influence of aluminum on IDH activity and protein levels.** *A*, activity staining of IDH on one-dimensional BN-PAGE is shown. *B*, Coomassie Blue staining of IDH on three-dimensional BN/BN/SDS-PAGE is shown. *C*, activity staining of soluble CFE for IDH on BN-PAGE is shown. *Lanes 1*, control; *2*, cells from control media transferred to aluminum-stressed media; *3*, cells from control media transferred to aluminum-stressed media with 50 μg/ml rifampicin; *4*, cells from control media transferred to aluminum-stressed media with 50 μg/ml chloramphenicol. *I* and *II*, IDH-NADP$^+$ isoenzymes.

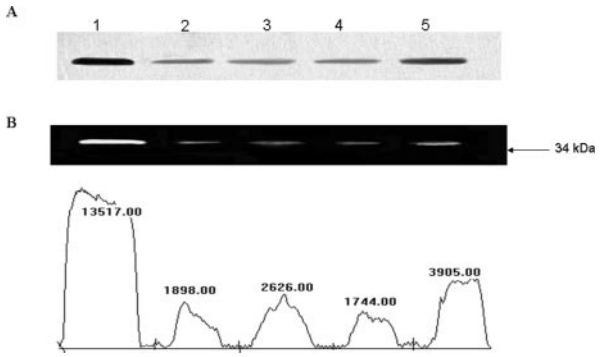

FIG. 7. **Influence of aluminum on ICL activity and protein levels.** *A*, activity stain of soluble CFE for ICL on BN-PAGE is shown. *B*, immunoblot for ICL using SDS-PAGE. *Lane 1*, cells from aluminum citrate medium; *lane 2*, cells from *1* incubated for 4 h in media devoid of aluminum (control media); *lane 3*, cells from *lane 2* incubated (6 h) in fresh aluminum citrate media containing rifampicin (200 μg/ml); *lane 4*, cells from *lane 2* incubated (6 h) in fresh aluminum citrate media containing chloramphenicol (200 μg/ml); *lane 5*, cells from *lane 2* incubated (6 h) in fresh aluminum citrate media devoid of protein synthesis inhibitors. Immunoblot band intensities were measured using SCION image software.

citrate and citrate with 25 μM Fe. However, in the cultures with H_2O_2, no significant improvement in Acn activity was evident, thus indicating the susceptibility of Acn to oxidative stress. Although the amount of protein corresponding to Acn was not affected in the presence of either chloramphenicol or rifampicin, the enzymatic activity was absent. Because the level of Acn expression was unaffected and Acn activity recovered in iron-cultured cells, studies were initiated to elucidate the significance of the Fe-S cluster in modulating Acn activity in aluminum-stressed cells. When Acn activity was measured after the incubation of the soluble CFE with $Fe(NH_4)_2(SO_4)_2$ and DTT, there was an increase of at least 2-fold in aluminum-stressed cells. No significant change was observed in the control cells (data not shown). The spectrophotometric scanning studies revealed spectra consistent with Fe-S cluster perturbation (Fig. 5*B*). The absorption band between 395 and 420 nm that has been shown to be characteristic of [4Fe-4S] (24, 25) clusters was markedly different in control than in aluminum-stressed CFE. In the former case, the band was sharp, whereas in the latter, a significant disruption in the band was evident. The sharpness of this band decreased with increasing concentration of aluminum in the growth medium. However, in CFE obtained from aluminum-stressed cells transferred to a medium devoid of the test metal, the distinctive band reappeared.

Effects of Aluminum on the Activity and Expression of IDH and ICL in P. fluorescens—IDH-NADP$^+$, an enzyme involved in the decarboxylation of isocitrate to α-ketoglutarate with concomitant formation of NADPH showed a higher activity in the CFE isolated from the aluminum-stressed cells compared with the control cells. Coomassie Blue staining of IDH on three-dimensional BN/BN/SDS-PAGE demonstrated higher levels of protein associated with IDH in the aluminum-stressed cells compared with the control cells (Fig. 6, *A* and *B*). Furthermore, an isoenzyme of IDH also was prominent in the aluminum-stressed cultures. The cells grown in the control medium were transferred into media supplemented with aluminum, aluminum with rifampicin, and aluminum with chloramphenicol. In the aluminum medium, a marked increase was observed after 8 h of incubation. However, in the aluminum media with chloramphenicol and rifampicin, no significant increase was recorded (Fig. 6*C*). ICL, another cytoplasmic enzyme known to cleave isocitrate (a product of Acn) to succinate and glyoxylate, was also found to undergo a marked increase in the aluminum-stressed cultures. The susceptibility of ICL to aluminum and its overexpression in the aluminum-stressed cells were also demonstrated by BN-PAGE and Western blot analyses (Fig. 7).

Degradation of Citrate to Glyoxylate and α-Ketoglutarate by the Soluble CFE from Control and Aluminum-stressed P. fluorescens—The soluble CFE was incubated with citrate, and the production of glyoxylate was quantitated. As depicted in Table I, the amounts of glyoxylate produced by both control and aluminum-stressed soluble fractions were relatively similar even though Acn activity in the aluminum-stressed cultures was severely inhibited. Likewise, the total α-ketoacid (*i.e.* glyoxylate and α-ketoglutarate generated by the soluble CFE from control and aluminum-stressed cultures) did not appear to vary significantly. The augmentation of ICL and IDH activities seemed to compensate for the drastic reduction of Acn activity observed in the cells subjected to aluminum stress.

DISCUSSION

The foregoing data show the pivotal role that ICL and IDH played in the adaptation of *P. fluorescens* when the organism was subjected to aluminum as a toxicant and citrate as the sole carbon source. The inhibitory influence of aluminum on the critical enzyme Acn *in vivo* was also demonstrated. The decrease in Acn activity was sensitive to the concentration of aluminum in the medium and was caused not by a decrease in protein expression but by the perturbation of the Fe-S cluster. Hence, Acn was a target of the toxic properties exhibited directly or indirectly by aluminum, with severe metabolic consequences. However, survival was assured not by an alternative citrate-degrading enzyme but rather by the overexpression of ICL and IDH, two enzymes acting downstream of Acn. The absence of any discernable amounts of citrate-lyase or ATP citrate-lyase clearly indicated that these enzymes are not involved in the decomposition of citrate (27). In this instance, Acn seemed to be the main enzyme participating in the decomposition of citrate, even though it is a target of aluminum toxicity. The ability of aluminum to mimic iron and generate reactive oxygen species creates an unfavorable environment for Acn to operate as an enzyme (14). This oxidative and iron-starved situation promoted by aluminum confers an unstable Acn with less than optimal activity. Indeed, it has been reported (28, 29)

TABLE I
Metabolism of citrate to aconitate, glyoxylate, and α-ketoglutarate in P. fluorescens

Enzymes monitored	Substrate	Product	Specific activity	
			A-stressed cells	Control cells
			nmol·min^{-1}·mg protein^{-1}	
Acn	Citrate	Aconitate	18 ± 15	124 ± 10
ICL	Isocitrate	Glyoxylate	54.9 ± 8	11.0 ± 6
IDH[a]	Isocitrate, $NADP^+$	α-Ketoglutarate	54 ± 2	35 ± 3
Acn, ICL	Citrate	Glyoxylate	8.38 ± 2	7.59 ± 3.2
Acn, IDH	Citrate, $NADP^+$[a]	α-Ketoglutarate	29 ± 2	33 ± 2
Acn, ICL, and IDH	Citrate	Glyoxylate, α-Ketoglutarate	39 ± 1	34 ± 2

[a] 5 mM malonate was utilized as an inhibitor of ICL.

that the sensitivity of Acn to these conditions enables this protein to sense iron and oxygen tension and allows it to regulate the homeostasis of iron and energy. In the present study, the level of Acn in both the control and aluminum-stressed cultures were the same, but their activities were markedly disparate. The Acn from the aluminum-stressed bacteria had sharply diminished activity. This activity was partially restored on incubation with DTT and $Fe(NH_4)_2(SO_4)_2$ or when the aluminum-stressed cells were exposed to an iron-enriched medium. It is important to note that the level of activity in the aluminum-stressed culture was similar to the level observed in the medium containing glucose as the sole source of carbon. Hence, it is conceivable that although the activity was diminished in aluminum-stress, it was enough to support the decomposition of citrate. Indeed, Acn appeared overexpressed in the citrate cultures compared with expression in the medium with glucose. In *Escherichia coli*, the presence of AcnA and AcnB has been reported. It has been suggested that AcnB is sensitive to oxidative stress and participates in the tricarboxylic acid cycle during the earlier stages of growth, whereas AcnA is expressed more abundantly during the stationary phase (30, 31). In the present study, two-dimensional BN-PAGE and Western blot analyses revealed only one band corresponding to Acn activity. No Acn-like activity was discernable in any other cellular fractions analyzed. It is noteworthy that although Acn is sensitive to the presence of Ga^{3+} or H_2O_2 in the media, it is not affected by a redox-insensitive metal such as Ca^{2+}. Hence, an oxidative environment and a dearth of bioavailable iron triggered by aluminum might be the causative agents impeding Acn activity. It is also tempting to propose that Acn, in this instance, may also be serving as a stress-responsive switch involved in gauging the intracellular oxygen gradient and iron pool in bacteria. Such a role has been demonstrated recently (32). If Acn, with a markedly decreased activity, is the key enzyme routing citrate toward cellular metabolism in *P. fluorescens* exposed to aluminum citrate, then this metabolic strategy may be ineffective. Thus, it is not unlikely that other effectors may be recruited to assure the survivability of the microbe in this aluminum citrate environment. The physiological profile of the microbe in aluminum medium clearly points to the participation of other enzymes in this process (33). Indeed, the two enzymes ICL and IDH-$NADP^+$ that cleave isocitrate, the product of the isomerization of citrate by Acn, appear to be an integral part of the biochemical strategy invoked by *P. fluorescens* to survive this toxic challenge. ICL activity that increases 4-fold because of the overexpression of this protein is responsive to the presence of aluminum in the medium (34). The rapid decomposition of isocitrate will favor the conversion of citrate to isocitrate. The increased activity of ICL may also help supply glyoxylate, a pivotal contributor to the detoxification of aluminum. Indeed, glyoxylate is further oxidized to oxalic acid, a moiety that is involved in the sequestration of the trivalent metal (3). Hence, it is not unlikely that the up-regulation of ICL may be fulfilling the dual role of metabolizing citrate despite

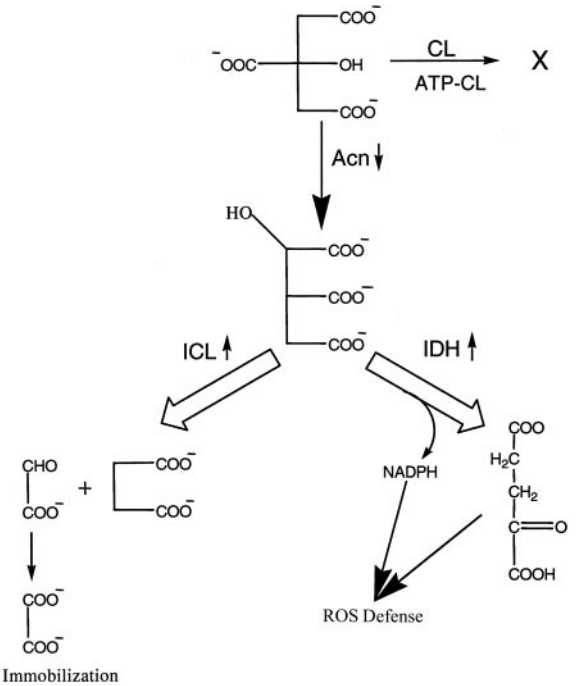

FIG. 8. **An aluminum-evoked metabolic network in *P. fluorescens*.** Increased activity and expression of ICL and IDH allow the degradation of citrate under decreased Acn activity. ↑, increased activity; ↓, decreased activity; *X*, undetected enzyme activity; *ROS*, reactive oxygen species.

low Acn activity and providing the key ingredient for the biogenesis of oxalic acid. This dicarboxylic acid has also been reported to act as an antioxidant (35), a situation that may be prevalent in the aluminum-stressed cells. Thus, by routing the flux of isocitrate toward its cleavage into glyoxylate and succinate, the up-regulation of ICL may favor the decomposition of citrate. Indeed, the ability of both the control and aluminum-stressed cells to generate similar amounts of glyoxylate from citrate clearly points to such a possibility *in vivo*.

IDH-$NADP^+$, which also utilizes isocitrate as a substrate, showed a marked increase in aluminum-stressed cells. This enhanced activity will have a beneficial effect on the conversion of citrate to isocitrate. The utilization of isocitrate will promote the further isomerization of citrate to isocitrate. This will, *de facto*, allow for the degradation of citrate even if the activity of Acn is diminished markedly because of the oxidative and iron-labile environment favored by aluminum stress. The diminished level of Acn activity in aluminum-stressed cells appeared to be mitigated by the up-regulation of the enzymes involved in the degradation of isocitrate. The overexpression of ICL and IDH in this instance may be fulfilling such a goal. Hence, a metabolic network that favors the channeling of substrates to be recruited for specific biological functions may be an important strategy that living systems invoke to adjust to changing

internal and external cellular environments. The inability and/or the inefficacy of alternative enzymes to metabolize citrate in an oxidative and iron-starved environment compels the cell to utilize a diminished Acn as the main mediator of citrate degradation. Furthermore, it is not unreasonable to hypothesize that this Acn with perturbation in its Fe-S cluster may be acting both as a regulatory and a diminished enzymatic moiety. This metabolic circuit involving Acn, IDH, and ICL allows for the degradation of citrate and generates the precursors that ensure survivability under aluminum stress. Indeed, NADPH and α-ketoglutarate may contribute to combating the oxidative tension generated by aluminum stress. In addition, glyoxylate, a product of ICL, enables the biogenesis of oxalic acid, a moiety involved in aluminum detoxification (Fig. 8). Thus, it is not inconceivable that the cell orchestrates a complete metabolic reconfiguration in an effort to deal with the abnormal situation imposed by aluminum stress. Metabolites are the eventual effectors of biological functions, and they allow the gauging of the biochemical status of an organism. They provide an insight into the metabolic network and the proteins responsible for their production and decomposition. Hence, Acn, ICL, IDH, glyoxylate, succinate, isocitrate, citrate, NADPH, and α-ketoglutarate are intricately linked as part of the global metabolic network operating in aluminum-stressed *P. fluorescens.*

In summary, these results demonstrate that Acn, a key enzyme in cellular energy production, is a critical target of aluminum toxicity. The decreased Acn activity is not accompanied by a decrease in protein concentration but rather by the perturbation of the Fe-S cluster. This raises the possibility that the tricarboxylic acid cycle may be compromised under the toxic influence of aluminum. In this instance, the survival of the microbe in the aluminum-stressed environment is ensured by the up-regulation of ICL and IDH, two enzymes that usually act downstream to Acn. The increased activities of these two enzymes are concomitant with the corresponding increase in the respective protein levels. The flux of isocitrate via ICL and IDH enables the degradation of citrate even under diminished Acn efficacy. This concerted approach invoking a variety of enzymes may provide an evolutionary advantage for the survival of this aluminum-stressed organism and reveals the versatility of metabolic pathways in targeting metabolites toward specific proteins aimed at executing a desired function. Metabolomic and proteomic studies currently underway will help provide a snapshot of the interplay and an integration of the global metabolic network operative in *P. fluorescens* challenged with aluminum.

Acknowledgments—We thank Drs. R. Eisenstein (University of Wisconsin) and K. Honer Zu Bentrup (Cornell University) for antibodies for Acn and ICL, respectively.

REFERENCES

1. Sanford, K., Soucaille, P., Whited, G., and Chotani, G. (2002) *Curr. Opin. Microbiol.* **5,** 318–322
2. Goodacre, R. (2004) *Drug Discov. Today* **9,** 260–261
3. Hamel, R., and Appanna, V. D. (2003) *Biochim. Biophys. Acta* **1619,** 70–76
4. Hamel, R. D., and Appanna, V. D. (2001) *J. Inorg. Biochem.* **87,** 1–8
5. Schneider, K., Dimroth, P., and Bott, M. (2000) *FEBS Lett.* **483,** 165–168
6. Adams, I. P., Dack, S., Dickinson, F. M., and Ratledge, C. (2002) *Biochim. Biophys. Acta* **1597,** 36–41
7. Elshourbagy, N. A., Near, J. C., Kmetz, P. J., Sathe, G. M., Southan, C., Strickler, J. E., Gross, M., Young, J. F., Wells, T. N., and Groot, P. H. (1990) *J. Biol. Chem.* **265,** 1430–1435
8. Tuhackova, Z., and Krivanek, J. (1996) *Biochem. Biophys. Res. Commun.* **218,** 61–66
9. Clark, D. P. (1990) *FEMS Microbiol. Lett.* **55,** 245–249
10. Fridovich, I. (1995) *Annu. Rev. Biochem.* **64,** 97–112
11. Beinert, H., Kennedy, M. C., and Stout, C. D. (1996) *Chem. Rev.* **96,** 2335–2374
12. Haile, D. J., Rouault, T. A., Harford, J. B., Kennedy, M. C., Blondin, G. A., Beinert, H., and Klausner, R. D. (1992) *Proc. Natl. Acad. Sci. U. S. A.* **89,** 11735–11739
13. Nayak, P. (2002) *Environ. Res.* **89,** 101–115
14. Exley, C. (2004) *Free Radic. Biol. Med.* **36,** 380–387
15. Appanna, V. D., and Hamel, R. D. (1999) *Recent Res. Dev. Microbiol.* **3,** 615–663
16. Ma, J. F., Zheng, S. J., Matsumoto, H., and Hiradale, S. (1997) *Nature* **390,** 559–560
17. Hamel, R., Levasseur, R., and Appanna, V. D. (1999) *J. Inorg. Biochem.* **76,** 99–104
18. Bradford, M. M. (1976) *Anal. Biochem.* **72,** 248–254
19. Henson, C. P., and Cleland, W. W. (1967) *J. Biol. Chem.* **242,** 3833–3838
20. Romanov, V., Merski, M. T., and Hausinger, R. P. (1999) *Anal. Biochem.* **268,** 49–53
21. Schagger, H., and von Jagow, G. (1991) *Anal. Biochem.* **199,** 223–231
22. Warren, W. A. (1970) *Biochim. Biophys. Acta* **212,** 503–505
23. Laemmli, U. K. (1970) *Nature* **227,** 680–685
24. Soum, E., Brazzolotto, X., Goussias, C., Bouton, C., Moulis, J. M., Mattioli, T. A., and Drapier, J. C. (2003) *Biochemistry* **42,** 7648–7654
25. Berndt, C., Lillig, C. H., Wollenberg, M., Bill, E., Mansilla, M. C., de Mendoza, D., Seidler, A., and Schwenn, J. D. (2004) *J. Biol. Chem.* **279,** 7850–7855
26. Conover, W. W. (1984) in *Topics in Carbon-13 NMR Spectroscopy* (Levy, G. C., ed) Vol. 4, p. 4, John Wiley & Sons, NY
27. Hamel, R. (2003) in *Enhanced Lipogenesis and Oxalogenesis in Pseudomonas fluorescens Exposed to Aluminum Stress: A Study of Intermediary Metabolism.* Department of Chemistry and Biochemistry, University of Waterloo, Waterloo, Ontario, Canada
28. Cairo, G., Recalcati, S., Pietrangelo, A., and Minotti, G. (2002) *Free Radic. Biol. Med.* **32,** 1237–1243
29. Eisenstein, R. S. (2000) *Annu. Rev. Nutr.* **20,** 627–662
30. Gruer, M. J., and Guest, J. R. (1994) *Microbiology* **140,** 2531–2541
31. Varghese, S., Tang, Y., and Imlay, J. A. (2003) *J. Bacteriol.* **185,** 221–230
32. Alen, C., and Sonenshein, A. L. (1999) *Proc. Natl. Acad. Sci. U. S. A.* **96,** 10412–10417
33. Appanna, V. D., Huang, J., Prusak-Sochaczewski, E., and St. Pierre, M. (1995) *Biotechnol. Prog.* **11,** 159–166
34. Hamel, R., Appanna, V. D., Viswanatha, T., and Puiseux-Dao, S. (2004) *Biochem. Biophys. Res. Commun.* **317,** 1189–1194
35. Kayashima, T., and Katayama, T. (2002) *Biochim. Biophys. Acta* **1573,** 1–3